



Cite this: DOI: 10.1039/c8ce01152d

# Cooperative structure direction of organosilanes and tetrapropylammonium hydroxide to generate hierarchical ZSM-5 zeolite with controlled porous structure†

 Yu Shen, <sup>a</sup> Zongzhuang Han, <sup>a</sup> Hang Li, <sup>a</sup> Haichao Li, <sup>b</sup> Gang Wang, <sup>b</sup> Fumin Wang <sup>\*a</sup> and Xubin Zhang <sup>\*a</sup>

Hierarchical ZSM-5 zeolite with short-range ordered mesoporosity and hierarchical ZSM-5 zeolite nanorods were obtained *via* a direct hydrothermal synthesis by the cooperative structure direction of dimethyloctadecyl[3-(trimethoxysilyl)propyl]- ammonium chloride (TPOAC) and tetrapropylammonium hydroxide (TPAOH). Dimethyloctadecyl[3-(dimethoxymethylsilyl)propyl]ammonium chloride (DPOAC) and octadecyltrimethylammonium chloride (OTAC) were also employed as structure directing agents (SDA) to further explore the role of methoxysilyl groups in organosilanes during the formation of hierarchical structure. The prepared materials were characterized by X-ray diffraction (XRD), scanning electron microscope (SEM), transmission electron microscope (TEM), N<sub>2</sub> adsorption-desorption, FT-IR, UV-vis and inductively coupled plasma-optical emission spectroscopy (ICP-OES). The characterization results showed that the use of TPOAC and DPOAC would generate short-range ordered mesopores and irregular mesopores, respectively. Hierarchical ZSM-5 zeolite nanorods with worm-like intracrystalline mesopores could be obtained by adjusting the amount of silicon source. The lack of methoxysilyl groups in OTAC however could lead to phase separation problems. Furthermore, the hierarchical Fe-ZSM-5 zeolite with short-range ordered mesoporosity showed enhanced catalytic activity and stability for the hydroxylation of phenol at room temperature.

 Received 13th July 2018,  
Accepted 10th September 2018

DOI: 10.1039/c8ce01152d

[rsc.li/crystengcomm](http://rsc.li/crystengcomm)

## 1. Introduction

ZSM-5 zeolites are crystalline aluminosilicates with regular microporosity containing tetrahedral TO<sub>4</sub> (T represents Si or Al) structure and MFI topology, which is composed of two crossing channels (0.53 nm × 0.56 nm, 0.51 nm × 0.55 nm) with 10-membered ring openings: one is a straight channel parallel to the [010] crystal plane and the other is a sinusoidal channel parallel to the [001] crystal plane.<sup>1–3</sup> The unique framework in ZSM-5 zeolites brings about high surface areas, excellent shape selectivity and great hydrothermal stability, as a result of which they are extensively employed as catalysts or catalyst supports in industry. However, the micropores of the MFI structure in ZSM-5 zeolites lead to diffusion limitations and further inhibit their full utilization in catalysis, especially

when the kinetic diameter of reactants is bigger than those of the micropores. ZSM-5 zeolites can be considered to be promising catalysts for macromolecular reactants if the mass transfer is extensively improved.

From the viewpoint of catalytic materials design, the enhancement of the diffusion property for ZSM-5 zeolites can be achieved by creating hierarchical structure or decreasing the crystal size in one or more dimensions. The emergence of hierarchical structure in ZSM-5 zeolites could provide better diffusion properties, high accessibility, and superior catalytic performance than that of conventional zeolites with only micropores.<sup>4–7</sup> In addition, an improved resistance to coking with increasing external (mesopore) surface area can be envisaged due to the facilitated escape of coke precursors and the larger area that needs to be covered to block access to the micropores.

So far, the construction of hierarchical structure in zeolites could be realized *via* two general strategies: top-down and bottom-up routes.<sup>8</sup> The typical top-down route<sup>9–14</sup> is the removal of framework atoms by post-treatment techniques such as desilication and dealumination, while the bottom-up route can be classified as hard-templates,<sup>15–18</sup> soft-

<sup>a</sup> School of Chemical Engineering and Technology, Tianjin University, Tianjin, China. E-mail: wangfumin@tju.edu.cn, tjzxb@tju.edu.cn; Tel: +86 139 2000 0387, +86 138 2168 4327

<sup>b</sup> School of Chemistry and Chemical Engineering, Qinghai Nationalities University, Xining, China

† Electronic supplementary information (ESI) available. See DOI: 10.1039/c8ce01152d

templates<sup>19–31</sup> and template-free methods.<sup>32,33</sup> Among them, the soft-templates method is recognized as the most innovative approach, because both the mesoporous structure and microporous framework type can be easily controlled *via* the use of surfactants with different molecular structure. During the crystallization process, however, the phase-separation phenomenon between the surfactants and aluminosilicate domains will lead to the generation of physical mixtures of amorphous material without microporosity and bulk zeolite with only micropores, which could impose difficulties for the surfactants to modulate the zeolite crystal growth into a hierarchical structure. Choi *et al.*<sup>22</sup> reported that hierarchical ZSM-5 zeolites could be obtained *via* an organosilane surfactant with hydrophobic alkyl chain and hydrolysable methoxysilyl groups as mesoporous structure-directing agents (SDA). Methoxysilyl groups played a very important role for overcoming the phase-separation problem due to the strong interaction between the hydrolysable methoxysilyl groups and growing crystal domains. Thereafter, this kind of organosilane has been extensively used as mesoporous SDA for the synthesis of hierarchical zeolites.<sup>34–40</sup> Milina *et al.*<sup>41</sup> corroborated the concept of mesopore quality through the connectivity as well as lifetime of the catalysts. The results show that catalysts obtained *via* organosilane possess constricted mesopores rather than open and interconnected mesopores. Thus, to design a superior hierarchical zeolite catalyst, at least two factors should be significantly considered: one is to find or synthesize a soft-template to prevent phase-separation phenomenon during the crystallization process, the other is to construct mesopores with good quality, which can provide better mass transfer, accessibility and lifetime than the conventional hierarchical structure can. However, the works related to hierarchical ZSM-5 zeolites by using organosilanes as SDA are mainly focused on the synthesis of conventional hierarchical structure. The one-step hydrothermal synthesis of hierarchical ZSM-5 zeolite with controlled porous structure still needs to be investigated further.

Herein, to further improve the mesopore quality, we report a one-step synthesis route to prepare hierarchical ZSM-5 zeolite with short-range ordered mesoporosity and hierarchical ZSM-5 zeolite nanorods by the cooperative structure direction of organosilane and tetrapropylammonium hydroxide. The synthesized materials can be considered as typical catalysts which combine shorter length of diffusion path and micro-mesoporous structure into one unit, that in turn will promote the diffusion of reactants and products in and out of the catalyst particles, as well as the accessibility of the active sites for reactants and intermediate products. Furthermore, the effect of the amount of hydrolysable methoxysilyl groups on the hierarchical structure is further discussed based on the characterization results by using DPOAC as the SDA (Scheme S1, ESI<sup>†</sup>). To verify the mesopore quality, ferric iron was introduced into the framework as active sites for the hydroxylation of phenol. The great catalytic properties of the Fe-substituted hierarchical ZSM-5 sample showed remarkably enhanced catalytic activity and stability for the hydroxylation of phenol.

## 2. Experimental section

### 2.1 Materials

Sodium hydroxide (NaOH, 99%), tetraethyl orthosilicate (TEOS, 99%), octadecyltrimethylammonium chloride (OTAC, 99%), tetrapropylammonium hydroxide (TPAOH, 25 wt% in water), sodium metaaluminate (NaAlO<sub>2</sub>, 99%), methanol (99%), ethanol (99%), iron chloride hexahydrate (FeCl<sub>3</sub>·6H<sub>2</sub>O, 99%), phenol (99%), catechol (CAT, 99%), hydroquinone (HQ, 99%), benzoquinone (BQ, 99%), ethylbenzene (EB, 99%), H<sub>2</sub>O<sub>2</sub> (30 wt%), were purchased from Aladdin Co., Ltd. and used without any further purification. Dimethyloctadecyl[3-(trimethoxysilyl)propyl]ammonium chloride (TPOAC, 60 wt% in methanol) was purchased from J&K Scientific Co., Ltd. dimethyloctadecyl[3-(dimethoxymethylsilyl)propyl]ammonium chloride (DPOAC, 60 wt% in methanol) was purchased from Nanxiong Dingcheng New Material Technology Co., Ltd. Prior to use, the concentration of H<sub>2</sub>O<sub>2</sub> was tested by direct iodine titration.

### 2.2 Synthesis of hierarchical ZSM-5

The hierarchical ZSM-5 zeolites were obtained *via* a single step hydrothermal method in the presence of organosilanes (DPOAC, TPOAC) and tetrapropylammonium hydroxide (TPAOH) as soft-templates. To obtain hierarchical ZSM-5 zeolites, TEOS and the organosilane surfactant dissolved in methanol were successively added to a mixture containing NaOH, TPAOH, NaAlO<sub>2</sub> and distilled water (molar ratios: 1 Al<sub>2</sub>O<sub>3</sub>:14 TPAOH:22.1 DPOAC/TPOAC:14 Na<sub>2</sub>O:8800 H<sub>2</sub>O:49 SiO<sub>2</sub>). In a typical procedure, 0.067 g NaAlO<sub>2</sub>, 4.2 g TPAOH and 0.41 g NaOH were first dissolved in 65 g H<sub>2</sub>O. Then, 4.2 g TEOS were slowly adding into the solution at room temperature. After stirring for 2 hours, a mixture of desired amount of DPOAC or TPOAC dissolved in methanol were added under vigorous stirring (500 rpm). The final mixture was further stirred for 2 hours. The mother liquid was then moved into a teflon-coated stainless-steel autoclave and heated at 150 °C for 72 hours. The obtained materials were separated by centrifuge, washed thrice with ethanol, dried at 80 °C overnight and calcined in air at 550 °C for 6 hours. The prepared materials were denoted as DH-ZSM-5(4.2) or TH-ZSM-5(4.2), respectively. TH-ZSM-5(6.3) was obtained with 6.3 g of TEOS. For the purpose of comparison, conventional ZSM-5 (ZSM-5) was prepared with the presence of only TPAOH. To obtain the Fe-substituted catalyst, desired amount of ferric chloride hexahydrate was added into the mother liquid after the addition of TEOS.

### 2.3 Characterization

X-ray diffraction (XRD) was tested by using a Bruker D8-Focus instrument with Ni-filtered Cu K $\alpha$  radiation ( $\lambda = 0.1541$  nm) with a scanning rate of 5° per minute in the range of 5–50°. The morphologies of the samples were observed by using a scanning electron microscopy (SEM, Hitachi S-4800) instrument operating at 20 kV. To ensure electrical conductivity, a thin platinum film was sprayed on the samples by using an

ion sputtering apparatus prior to taking any measurements. The hierarchical structures of the samples were recorded on a transmission electron microscopy (TEM, JEM-2100F) operating at 200 kV. Each sample was first dispersed in ethanol using an ultrasonic instrument and then dropped onto ultrathin carbon supported film before measurement.  $N_2$  sorption isotherms were measured at 77 K on a SSA-7000 (BUIDER, CH) instrument. Before measurements, all samples were degassed at 250 °C for 6 hours. The BET method was employed to measure the specific surface areas ( $S_{BET}$ ). The pore size distributions of micropores and mesopores were calculated by the Horvath–Kawazoe (HK) and Barrett–Joyner–Halenda (BJH) models (adsorption branch), respectively. Fourier transforming infrared spectra (FT-IR) were collected in the range of 4000  $cm^{-1}$  to 400  $cm^{-1}$  at room temperature on a Thermo Nicolet instrument by using the KBr pellet technique. The UV-vis spectra were recorded on a PE Lambda 750 spectrophotometer in the range of 200–600 nm. The Si/Fe ratios of the prepared samples were measured by inductively coupled plasma-optical emission spectrometry (ICP-OES, PerkinElmer) instrument.

#### 2.4 Catalyst activity

The hydroxylation of phenol was conducted in a three-necked flask (50 mL) with an electric stirring water bath under vigorous stirring (600 rpm). Typically, 1 g of phenol, 10 mL of deionized water and 0.1 g of catalyst were added into the three-necked flask at 25 °C. Then, desired amount of  $H_2O_2$  was added into the flask. After reaction, the catalysts were separated from reaction mixture by centrifugation. Gas chromatograph analyses were conducted by using a Shimadzu GC-2010 plus instrument equipped with a SE-30 chromatographic capillary column ( $\varnothing$  0.25 mm  $\times$  0.25  $\mu$ m  $\times$  30 m). Gas chromatography–mass spectrometry analyses were performed on a Shimadzu QP2010 instrument. Ethyl benzene was used as the internal standard to calculate the mass of reactant and products.

### 3. Results and discussion

The XRD patterns of TH-ZSM-5(4.2), TH-ZSM-5(6.3), DH-ZSM-5(4.2) and conventional ZSM-5 samples are shown in Fig. 1. TH-ZSM-5(4.2), TH-ZSM-5(6.3), DH-ZSM-5(4.2) and conventional ZSM-5 samples show characteristic peaks of a typical MFI zeolite framework, indicating that the hydrolysable methoxysilyl siloxane groups have no influence on the formation of MFI structure, which is in agreement with previous study.<sup>22</sup> The FT-IR spectra of the synthesized hierarchical ZSM-5 and conventional ZSM-5 samples show that two bands at 1088  $cm^{-1}$  and 1225  $cm^{-1}$  are characteristic of internal and external asymmetric stretching, respectively, while the band at 797  $cm^{-1}$  is caused by the external symmetric stretching (Fig. S1, ESI<sup>†</sup>).<sup>42</sup> The band observed at 546  $cm^{-1}$  can be attributed to the characteristic peak of the MFI structure.<sup>43</sup>

The SEM images of the four samples are shown in Fig. 2. As shown in the figure, conventional ZSM-5 prepared by the

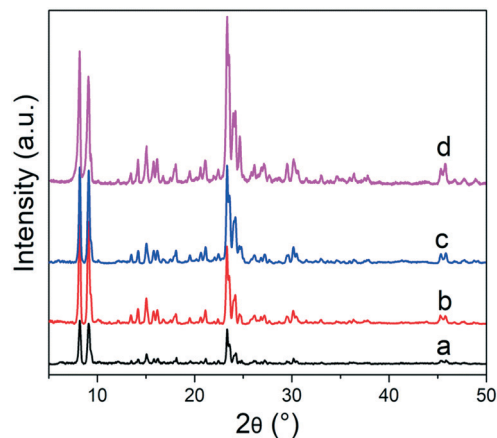


Fig. 1 The XRD patterns of (a) TH-ZSM-5(4.2); (b) DH-ZSM-5(4.2); (c) TH-ZSM-5(6.3); (d) conventional ZSM-5 samples.

solo presence of TPAOH shows bulky ZSM-5 zeolite crystals ( $>10 \mu$ m). The morphology changed when TPOAC were added into the mother liquid of ZSM-5 zeolite, indicating the occurrence of interaction between hydrolysable methoxysilyl siloxane groups in TPOAC and the growing crystal domains of the MFI structure.<sup>22</sup> TH-ZSM-5(4.2) shows obvious long narrow macropores with a rough surface, while TH-ZSM-5(6.3) results in a nanorod morphology. Each nanorod is about 50–100 nanometers in width. When DPOAC was replaced by TPOAC to synthesize hierarchical ZSM-5 zeolite, the macropores changed from long and narrow to smaller and irregular in the DH-ZSM-5(4.2) sample. This phenomenon may be because the two methoxysilyl groups in DPOAC provide less interaction with the growing crystal domains than the three methoxysilyl groups in TPOAC do.

Fig. 3 shows the TEM images of TH-ZSM-5(4.2), TH-ZSM-5(6.3), DH-ZSM-5(4.2) and conventional ZSM-5 samples. As shown in the figure, zeolitic micropores can be observed in conventional ZSM-5 sample, which could be assigned to the MFI structure. TEM images also show that TH-ZSM-5(4.2) possesses ordered micropores and short-range ordered mesopores, while DH-ZSM-5(4.2) gives irregular and disordered mesopores. Nanorod morphology can be found in the TH-ZSM-5(6.3) sample. Each nanorod has ordered micropores of MFI structure and worm-like intracrystalline mesopores. The unique hierarchical structure of good connectivity coupled with controllable porous structure may be advantageous to alleviate the diffusion limitations and facilitate reactions including macromolecular reactants. When the amount of silicon source was decreased to 2.1 g, the XRD pattern of TH-ZSM-5(2.1) sample shows no characteristic peak of MFI structure (Fig. S2, ESI<sup>†</sup>), indicating that the amount of silicon source is a key factor for the formation of hierarchical MFI zeolite through cooperative structure direction of organosilanes and TPAOH. This phenomenon confirms that organosilanes and TPAOH would also play a competitive role when less silicon sources were used. In order to further explore the cooperative mechanism of the two templates, the precursors of TH-ZSM-5(4.2), TH-ZSM-5(6.3), and DH-ZSM-5(4.2) samples stirred for

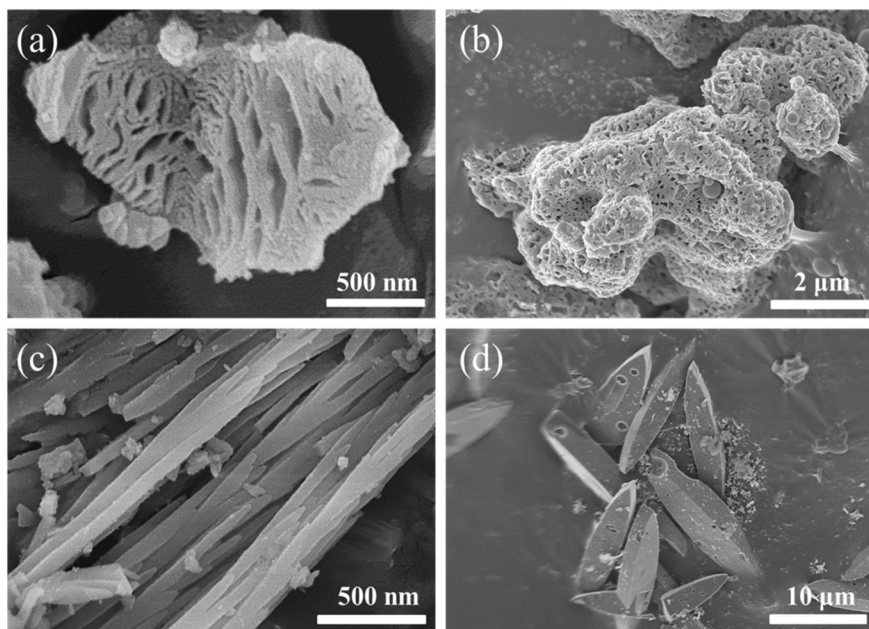


Fig. 2 The SEM images of (a) TH-ZSM-5(4.2); (b) DH-ZSM-5(4.2); (c) TH-ZSM-5(6.3); (d) conventional ZSM-5 samples.

different times before crystallization were collected by centrifugation, dried in a vacuum drying oven and characterized by TEM (Fig. 4). After stirring for two hours, no precursor of conventional ZSM-5 could be found and the mother liquor is pellucid. Precursors of the others samples could be collected as the mother liquids are white and turbid. This is probably caused because the prepolymers obtained from hydrolysis and condensation of silicon source were connected with the organosilanes by the hydrolysis of methoxysilyl groups.<sup>44,45</sup> Irregular mesopores and short-range ordered mesopores could be observed in the precursors of DH-ZSM-5(4.2) and TH-ZSM-5(4.2), respectively, which is in accordance with Fig. 3. Furthermore, the precursor of TH-ZSM-5(6.3) shows an approximately round morphology with narrow mesopores. These phenomena indicate that the mesoporous phase would be first formed at room temperature. Thus, when the amount of TEOS decreased to 2.1 g, the microporous phase will not be generated due to the lack of silicon sources.

$N_2$  adsorption–desorption isotherms (Fig. 5) and the pore size distributions (Fig. 6) of conventional ZSM-5 zeolite show obvious uptake of  $N_2$  at low relative pressure and type-I adsorption isotherms, confirming the solo presence of micropores. The strong adsorption at low relative pressure of TH-ZSM-5(4.2), TH-ZSM-5(6.3), DH-ZSM-5(4.2) and conventional ZSM-5 samples proves the presence of micropores in these hierarchical ZSM-5 zeolites. The size of the micropores, obtained from the Horvath Kawazoe (HK) model, was very similar in these samples, *ca.* 0.55 nm, suggesting the existence of the same type of micropores. The hysteresis in the adsorption isotherms could be ascribed to capillary condensation in mesopores.<sup>46</sup> According to the IUPAC classification, the combined features of type I at low relative pressure ( $P/P_0 < 0.01$ ) and a hysteresis with enhanced uptake in the region

of  $P/P_0 > 0.4$  in TH-ZSM-5(4.2), TH-ZSM-5(6.3) and DH-ZSM-5(4.2) samples confirm the presence of original micropores of MFI structure and newly created mesopores. Moreover, the pore size distributions (Fig. 6) clearly show the presence of mesopores in hierarchical ZSM-5 samples, with the mesopore size in the range of 2–15 nm. Table 1 exhibits the textural parameters of the prepared samples. It can be seen that the mesopore volume of the hierarchical ZSM-5 increases with the increasing amount of organosilanes, whereas the micropore volume decreases.

To further verify the role of methoxysilyl groups during crystallization, the material was also prepared by using octadecyltrimethylammonium chloride (OTAC) without methoxysilyl groups under the same conditions, denoted as OH-ZSM-5. The XRD pattern,  $N_2$  sorption isotherms, SEM image and TEM image were recorded as shown in Fig. 7. The XRD pattern shows the typical characteristic peak of the MFI structure, while the enhanced uptake of nitrogen in the relative pressure region of  $P/P_0 > 0.4$  of  $N_2$  sorption isotherms confirms the presence of mesopores. However, the SEM and TEM image indicate that the synthesized material is a physical mixture of MFI zeolite crystal and amorphous mesoporous silica material. This phenomenon demonstrates that methoxysilyl groups, which could provide interactions between the SDA and growing crystal domains through the formation of covalent bonds with other  $SiO_2$  and  $Al_2O_3$  sources,<sup>22</sup> played a significant role to overcome phase separation problem during the process of cooperative structure direction of the micropore- and mesopore-directing agents.

Few heterogeneous catalysts have been found to exhibit good catalytic performance in the hydroxylation of phenol at room temperature (25 °C). Lower reaction temperature is more conducive to extending catalyst life, but harmful to

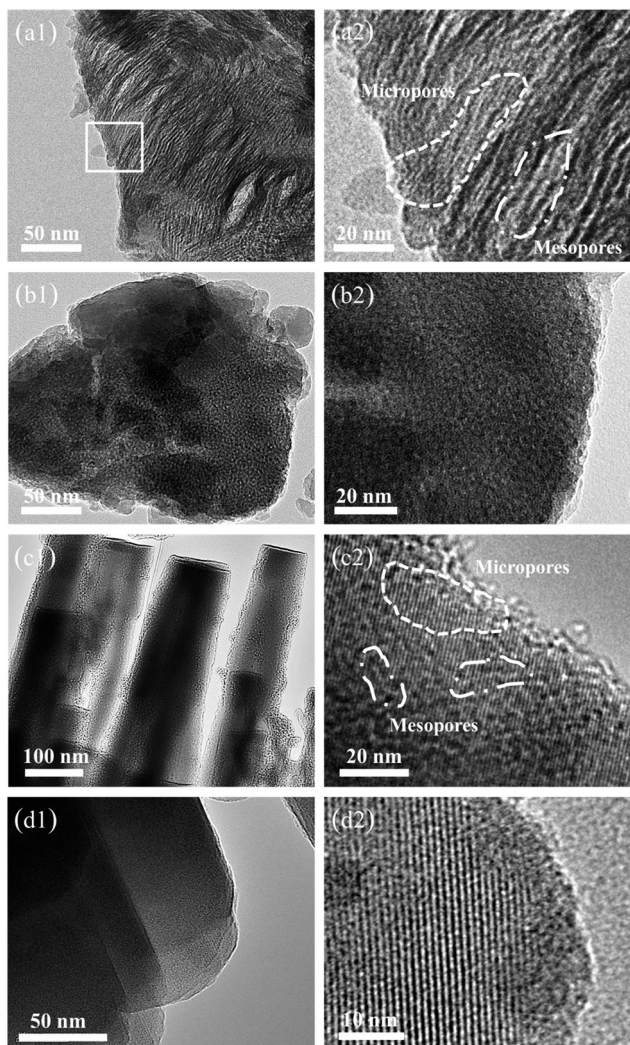


Fig. 3 The TEM images of (a1 and a2) TH-ZSM-5(4.2); (b1 and b2) DH-ZSM-5(4.2); (c1 and c2) TH-ZSM-5(6.3); (d1 and d2) conventional ZSM-5 samples.

catalytic conversion. According to the above analyses, the Fe-substituted hierarchical ZSM-5 catalysts with controllable porous structure could have high activity as the mass transfer and accessibility of the active sites is considered to be greatly improved. To catalyze the hydroxylation of phenol over the prepared hierarchical ZSM-5 zeolites, Fe-TH-ZSM-5(4.2), Fe-TH-ZSM-5(6.3), Fe-DH-ZSM-5(4.2) and conventional Fe-ZSM-5 were synthesized by adding the desired amount of ferric chloride hexahydrate into the mother liquid before crystallization while other conditions remained unchanged. A broad UV-vis absorption band (Fig. 8a) centered at 252 nm caused by  $d\pi\text{-}\pi$  charge transfer between tetrahedral oxygen ligands and  $\text{Fe}^{3+}$  ion prove that Fe-substituted catalysts were successfully synthesized.<sup>42</sup> The XRD patterns (Fig. 8b) of the prepared Fe-substituted samples also show a well-crystallized ZSM-5 structure, confirming that the substitution of iron has no effect on the MFI structure as well as the morphologies and pore structures shown in SEM images (Fig. S3, ESI<sup>†</sup>) and TEM im-

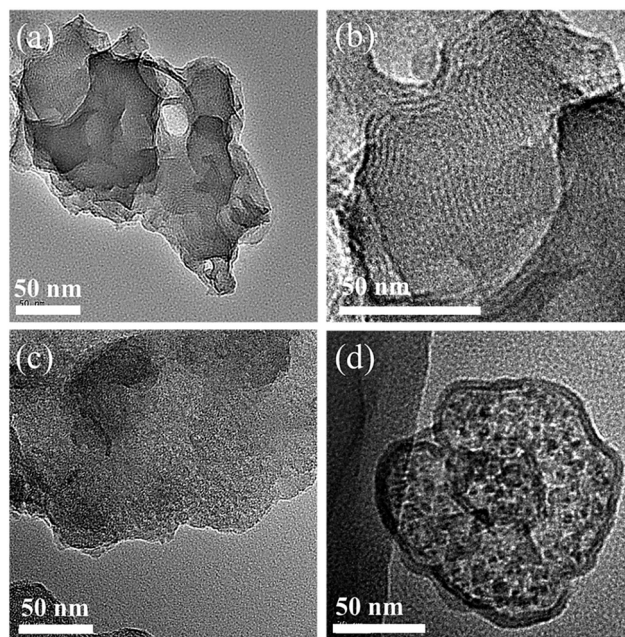


Fig. 4 The TEM images of the precursors of (a and b) TH-ZSM-5(4.2); (c) DH-ZSM-5(4.2); (d) TH-ZSM-5(6.3) samples.

ages (Fig. S4, ESI<sup>†</sup>). To test the pore structures further, the  $\text{N}_2$  adsorption-desorption isotherms, pore size distributions and textural properties of Fe-TH-ZSM-5(4.2), Fe-TH-ZSM-5(6.3), Fe-DH-ZSM-5(4.2) and conventional Fe-ZSM-5 were also measured as shown in Fig. S5 and Table S1 (ESI<sup>†</sup>). The characterization results also indicate that the pore sizes, pore volumes and BET areas slightly decreased when ion species were doped into the framework of the samples, which is in agreement with previous works.<sup>49,50</sup> According to the results of ICP-OES, the four samples have similar Fe content in solid (Table S1<sup>†</sup>). The catalytic activities of the prepared hierarchical ZSM-5 (Table 2) for the hydroxylation of phenol were compared with the conventional ZSM-5 at room temperature (reaction conditions: water 10 mL, catalyst 100 mg, phenol/ $\text{H}_2\text{O}_2$  molar ratio 2:1, 298 K, reaction time 12 h). As shown in

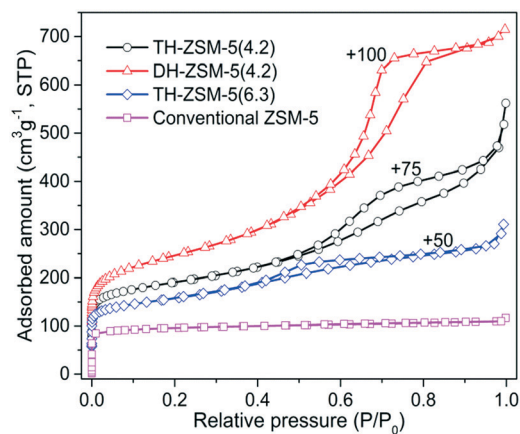


Fig. 5 The  $\text{N}_2$  adsorption-desorption isotherms of TH-ZSM-5(4.2), DH-ZSM-5(4.2), TH-ZSM-5(6.3) and conventional ZSM-5 samples.

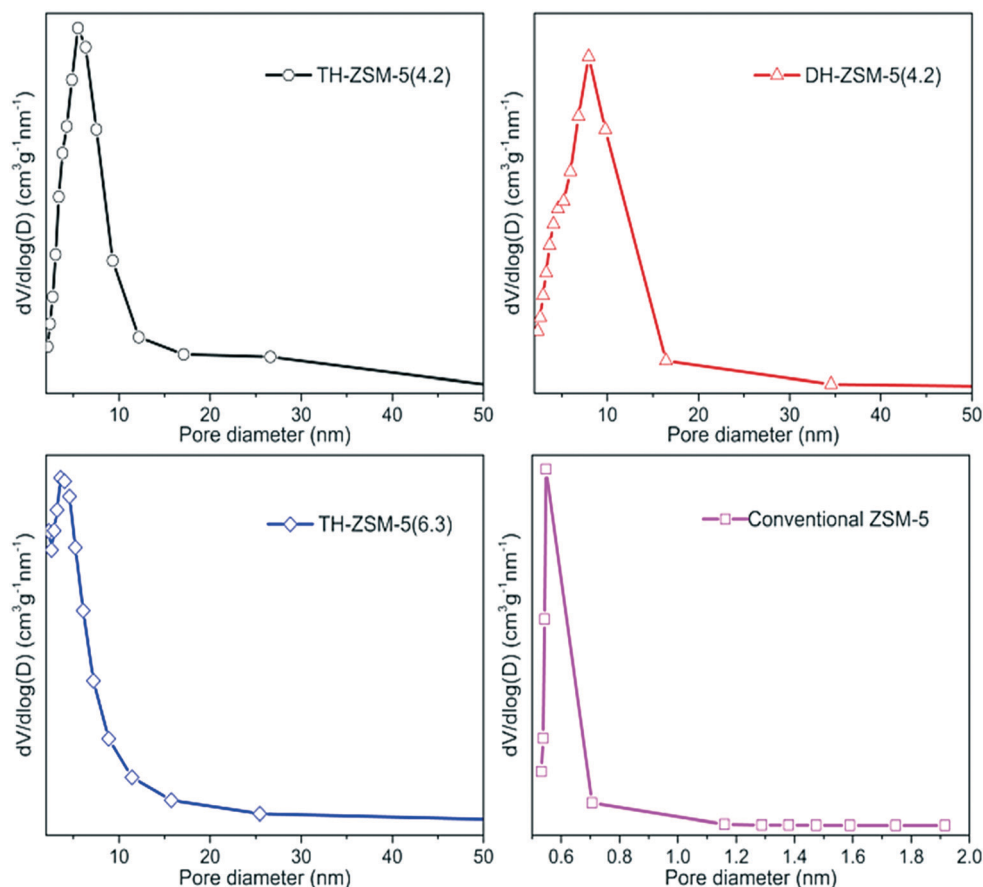


Fig. 6 The pore size distributions of TH-ZSM-5(4.2), DH-ZSM-5(4.2), TH-ZSM-5(6.3) and conventional ZSM-5 samples.

Table 1 Textural properties of TH-ZSM-5(4.2), DH-ZSM-5(4.2), TH-ZSM-5(6.3) and conventional ZSM-5 samples

Samples	Si/Al <sup>a</sup>	$S_{\text{BET}}^b$ [m <sup>2</sup> g <sup>-1</sup> ]	$S_{\text{micro}}^c$ [m <sup>2</sup> g <sup>-1</sup> ]	$V_{\text{micro}}^c$ [cm <sup>3</sup> g <sup>-1</sup> ]	$V_{\text{meso}}^d$ [cm <sup>3</sup> g <sup>-1</sup> ]
TH-ZSM-5(4.2)	25	450	69	0.035	0.25
DH-ZSM-5(4.2)	24	565	113	0.06	0.31
TH-ZSM-5(6.3)	24	432	128	0.07	0.21
Conventional ZSM-5	22	282	244	0.12	0.02

<sup>a</sup> Measured by ICP-OES. <sup>b</sup> Brunner–Emmet–Teller (BET) surface area. <sup>c</sup> Determined by *t*-plot method. <sup>d</sup> Pore volume in the range of 2–50 nm.

Table 2, the conventional Fe-ZSM-5 only gives 12.1% conversion of phenol and 65.4% selectivity to dihydroxybenzene, indicating that the bulk morphology (>10 μm) and small micropores largely restricted the catalytic activity, while other catalysts show significantly improved conversion and selectivity. It is possible that the lower activity of conventional Fe-ZSM-5 is due to the longer diffusion length of larger crystals compared to those of the hierarchical samples. The orders of the catalytic conversion over the Fe-substituted hierarchical ZSM-5 zeolites at the same reaction conditions are as follows: Fe-TH-ZSM-5(4.2) > Fe-TH-ZSM-5(6.3) > Fe-DH-ZSM-5(4.2). TH-ZSM-5(4.2) is completely inactive without the doping of Fe<sup>3+</sup>, indicating that the framework Fe is the active site for the hydroxylation of phenol. Moreover, Fe-TH-ZSM-5(4.2) prepared by TPOAC give 41.4% phenol conversion and 97.4% se-

lectivity to dihydroxybenzene, which is better than those reported in the literature.<sup>47,48</sup> According to the characterization, the cooperative structure direction of DPOAC and TPAOH would generate irregular and disordered mesopores, while Fe-TH-ZSM-5(4.2) prepared by TPOAC and TPAOH possesses short-range ordered mesoporosity. The superior connectivity of the hierarchical structure in Fe-TH-ZSM-5(4.2) sample could supply great diffusion performance and more accessible active sites for the reaction. The Fe-TH-ZSM-5(6.3) sample with hierarchical nanorods shows lower catalytic conversion than the Fe-TH-ZSM-5(4.2) sample did but still much higher than that of the conventional Fe-ZSM-5 zeolite. This phenomenon indicates that worm-like mesopores in each nanorod can provide shorter length of diffusion path and advantages for the hydroxylation of phenol.

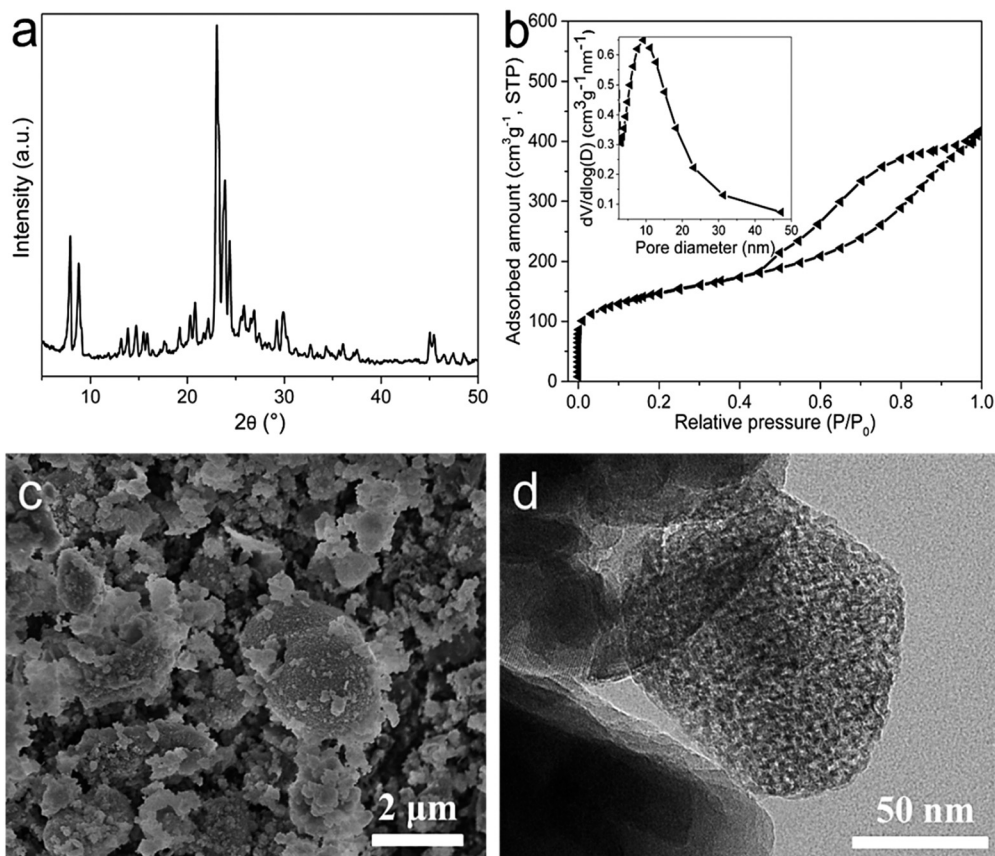


Fig. 7 (a) XRD spectrum, (b)  $N_2$  adsorption–desorption isotherm, (c) SEM image and (d) TEM image of OH-ZSM-5 sample prepared by using OTAC as mesopore-directing agent under the same conditions.

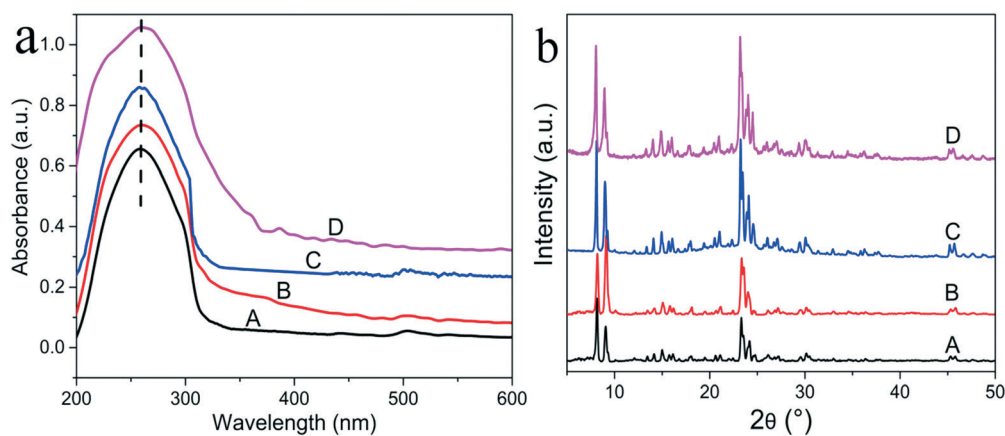


Fig. 8 (a) Uv-vis spectra and (b) XRD spectra of (A) Fe-TH-ZSM-5(4.2); (B) Fe-DH-ZSM-5(4.2); (C) Fe-TH-ZSM-5(6.3); (D) conventional Fe-ZSM-5 samples.

The catalytic stability of Fe-TH-ZSM-5(4.2) sample was tested under the same reaction conditions (Fig. 9). Before each cycle, the collected catalysts were washed by ethanol, dried and calcined in air. As shown in the figure, both the catalytic conversion and selectivity remain almost unchanged at room temperature after the reaction ran five times, indicating that Fe-TH-ZSM-5(4.2) sample has good reusability. In order to further verify the stability of the catalyst, the XRD pat-

tern and UV-vis absorption of the catalyst collected after fifth cycles, denoted as r-Fe-TH-ZSM-5, were recorded as shown in Fig. S6 (ESI<sup>†</sup>). The characterization results confirm that the MFI structure and framework Fe species remained almost unchanged. Furthermore, the molar ratios of Si/Fe after each cycle were tested as shown in Fig. 9, proving that there are no significant losses in the Fe content after undergoing the reactions. These phenomena demonstrate that the Fe-

**Table 2** The activity of hydroxylation of phenol over the Fe-substituted hierarchical ZSM-5 catalysts<sup>a</sup>

Catalyst	<sup>b</sup> Si/Fe	<sup>c</sup> Phenol/H <sub>2</sub> O <sub>2</sub>	$X_{\text{Phenol}}$ (%)	Selectivity (%)		$S_{\text{DHB}}$ (%)
				CAT	HQ	
Fe-TH-ZSM-5(4.2)	128	2:1	41.4	57.9	39.5	97.4
Fe-DH-ZSM-5(4.2)	126	2:1	39.3	48.9	36.8	85.7
Fe-TH-ZSM-5(6.3)	130	2:1	36.3	58.2	31.9	90.1
Conventional Fe-ZSM-5	126	2:1	12.1	43.2	22.2	65.4
TH-ZSM-5(4.2)	128	2:1	0	0	0	0
Fe-TH-ZSM-5(4.2)	128	3:1	22.7	60.5	37.4	97.9
Fe-TH-ZSM-5(4.2)	128	1:1	62.7	39.8	43.1	82.9
Fe-MCM41 <sup>d</sup>	11	3:1	25.3	?	?	78.4
FeCoNaβ <sup>e</sup>	1.12 <sup>f</sup>	3:1	21.4	49.4	16.7	66.1

<sup>a</sup> Reaction conditions: reaction temperature 25 °C, reaction time 12 h, 1 g of phenol, 10 g of water, 0.1 g of catalyst. <sup>b</sup> Molar ratio of Si to Fe, determined by ICP-OES. <sup>c</sup> Molar ratio of phenol to H<sub>2</sub>O<sub>2</sub>. <sup>d</sup> From ref. 47, reaction temperature 25 °C, phenol/H<sub>2</sub>O<sub>2</sub> (molar ratio) = 3, 1 g of phenol, 8.4 g of water, 0.05 g of catalyst. <sup>e</sup> From ref. 48, reaction temperature 30 °C, phenol/H<sub>2</sub>O<sub>2</sub> (molar ratio) = 3, 2 g of phenol, 60 g of water, 0.2 g of catalyst. <sup>f</sup> Fe content in mass (wt%).

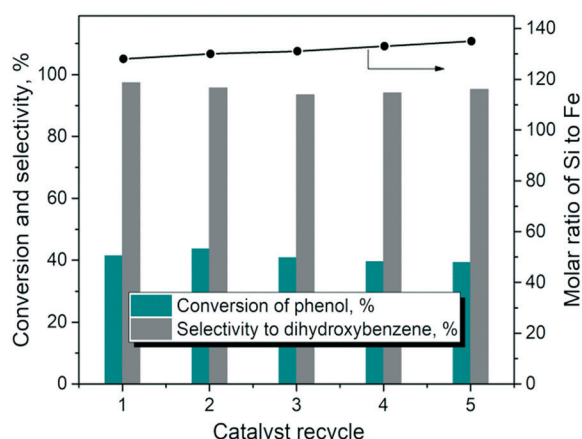


**Fig. 9** Catalytic stability of the Fe-TH-ZSM-5(4.2) sample. Reaction conditions: Reaction temperature 25 °C, reaction time 12 h, 1 g of phenol, 10 g of water, 0.1 g of catalyst.

substituted hierarchical ZSM-5 zeolite with short-range ordered mesoporosity has great catalytic stability.

## 4. Conclusion

In summary, hierarchical ZSM-5 zeolites with controlled porous structure have been successfully synthesized *via* a facile one-step hydrothermal route by the cooperative structure direction of organosilanes and tetrapropylammonium hydroxide. XRD, SEM, TEM and N<sub>2</sub> adsorption-desorption investigations revealed that hierarchical ZSM-5 with short-range ordered mesoporosity and hierarchical ZSM-5 nanorods with worm-like intracrystalline mesopores were successfully synthesized by adjusting the amount of silicon source in the presence of TPOAC. These hierarchical structures have two levels of porosity: one is the zeolitic microporosity arising from the crystalline structure, the other is the mesoporosity created by the organosilane template. The use of DPOAC could generate hierarchical ZSM-5 with irregular mesopores, while OTAC without methoxysilyl groups could cause a phase separation problem, indicating that the strong interaction be-

tween mesopore-directing agent and growing aluminosilicate domains obtained *via* the generation of covalent bonds with other SiO<sub>2</sub> and Al<sub>2</sub>O<sub>3</sub> sources is necessary. The Fe-substituted hierarchical ZSM-5 zeolite prepared by the cooperative structure direction of TPOAC and TPAOH showed superior catalytic performance at room temperature, which is better than most reported works, probably caused by the accelerated mass transfer and more accessible active sites. The strategy for the control of hierarchical structure in ZSM-5 zeolite demonstrated in this work might be useful as a principle for the design of other hierarchical zeolites.

## Conflicts of interest

There are no conflicts to declare.

## Acknowledgements

This work was supported by the National Basic Research Program of China (973 Program) (Grant no.2012CB720302) and the National Key Research and Development Program of China (2016YFF0102503).

## References

- G. T. Kokotailo, S. L. Lawton, D. H. Olson and W. M. Meier, *Nature*, 1978, 272, 437.
- Y. Wei, P. E. de Jongh, M. L. M. Bonati, D. J. Law, G. J. Sunleyb and K. P. de Jong, *Appl. Catal., A*, 2015, 504, 211.
- C. Pagis, A. R. M. Prates, D. Farrusseng, N. Bats and A. Tuel, *Chem. Mater.*, 2016, 28, 5205.
- C. M. A. Parlett, K. Wilson and A. F. Lee, *Chem. Soc. Rev.*, 2013, 42, 3876.
- Y. Wei, T. E. Parmentier, K. P. de Jong and J. Zecevic, *Chem. Soc. Rev.*, 2015, 44, 7234.
- Q. Sun, N. Wang, D. Xi, M. Yang and J. Yu, *Chem. Commun.*, 2014, 50, 6502.
- E. Verheyen, C. Jo, M. Kurttepel, G. Vanbutsele, E. Gobechiya, T. I. Korányi, S. Bals, G. V. Tendeloo, R. Ryoo, C. E. A. Kirschhock and J. A. Martens, *J. Catal.*, 2013, 300, 70.

- 8 K. A. Cychosz, R. Guillet-Nicolas, J. García-Martínez and M. Thommes, *Chem. Soc. Rev.*, 2017, **46**, 389.
- 9 J. C. Groen, W. D. Zhu, S. Brouwer, S. J. Huynink, F. O. Kapteijn, J. A. Moulijn and J. Pérez-Ramírez, *J. Am. Chem. Soc.*, 2007, **129**, 355.
- 10 J. C. Groen and J. A. Moulijn, *J. Mater. Chem.*, 2006, **16**, 2121.
- 11 J. C. Groen, L. A. Peffer, J. A. Moulijn and J. Pérez-Ramírez, *Chem. – Eur. J.*, 2005, **11**, 4983.
- 12 K. P. de Jong, J. Zečević, H. Friedrich, P. E. de Jongh, M. Bulut, S. van Donk, R. Kenmogne, A. Finiels, V. Hulea and F. Fajula, *Angew. Chem.*, 2010, **122**, 10272.
- 13 D. Verboekend, G. Vilé and J. Pérez-Ramírez, *Adv. Funct. Mater.*, 2012, **22**, 916.
- 14 S. J. Huang, X. H. Liu, L. L. Yu, S. Miao, Z. N. Liu, S. Zhang, S. J. Xie and L. Y. Xu, *Microporous Mesoporous Mater.*, 2014, **191**, 18.
- 15 C. J. H. Jacobsen, C. Madsen, J. Houzvicka, I. Schmidt and A. Carlsson, *J. Am. Chem. Soc.*, 2000, **122**, 7116–7117.
- 16 A. Boisen, I. Schmidt, A. Carlsson, S. Dahl, M. Brorson and C. J. Jacobsen, *Chem. Commun.*, 2003, 958.
- 17 J. Y. Liu, J. G. Wang, N. Li, H. Zhao, H. J. Zhou, P. C. Sun and T. H. Chen, *Langmuir*, 2012, **28**, 8600.
- 18 C. Y. Dai, A. F. Zhang, M. Liu and C. S. Song, *Adv. Funct. Mater.*, 2016, **25**, 7479.
- 19 Y. Cheneviere, F. Chieux, V. Caps and A. Tuel, *J. Catal.*, 2010, **269**, 161.
- 20 J. J. Jin, X. X. Ye, Y. S. Li, Y. Q. Wang, L. Li, J. L. Gu, W. R. Zhao and J. L. Shi, *Dalton Trans.*, 2014, **43**, 8196.
- 21 D. L. Yuan, C. Y. Kang, W. N. Wang and B. J. Shen, *Catal. Sci. Technol.*, 2016, **6**, 8364.
- 22 M. Choi, H. S. Cho, R. Srivastava, C. Venkatesan, D. H. Chio and R. Ryoo, *Nat. Mater.*, 2006, **5**, 718.
- 23 V. R. Reddy Marthala, L. Urmoneit, Z. Zhou, A. G. F. Machoke, M. Schmieles, T. Unruh, W. Schwieger and M. Hartmann, *Dalton Trans.*, 2017, **46**, 4165.
- 24 J. Zhu, Y. Zhu, L. Zhu, M. Rigutto, A. van der Made, C. Yang, P. Pan, L. Wang, L. Zhu, Y. Jin, Q. Sun, Q. Wu, X. Meng, D. Zhang, Y. Han, J. Li, Y. Chu, A. Zheng, S. Qiu, X. Zheng and F. S. Xiao, *J. Am. Chem. Soc.*, 2014, **136**, 2503.
- 25 S. T. Du, Q. M. Sun, N. Wang, X. X. Chen, M. J. Jia and J. H. Yu, *J. Mater. Chem. A*, 2017, **5**, 7992.
- 26 U. Diaz and A. Corma, *Dalton Trans.*, 2014, **43**, 10292.
- 27 M. Choi, K. Na, J. Kim, Y. Sakamoto, O. Terasaki and R. Ryoo, *Nature*, 2009, **461**, 246.
- 28 K. Na, C. Jo, J. Kim, K. Cho, J. Jung, Y. Seo, R. J. Messinger, B. F. Chmelka and R. Ryoo, *Science*, 2011, **333**, 328.
- 29 X. Y. Zhang, D. X. Liu, D. D. Xu, S. S. Asahina, K. A. Cychosz, K. V. Agrawal, Y. A. Wahedi, A. Bhan, S. A. Hashimi, O. Terasaki, M. Thommes and M. Tsapatsis, *Science*, 2012, **336**, 1684.
- 30 (a) Q. W. Tian, Z. H. Liu, Y. H. Zhu, X. L. Dong, Y. Saih, J.-M. Basset, M. Sun, W. Xu, L. k. Zhu, D. L. Zhang, J. F. Huang, X. J. Meng, F. S. Xiao and Y. Han, *Adv. Funct. Mater.*, 2016, **26**, 1881; (b) D. D. Xu, Y. H. Ma, Z. F. Jing, L. Han, B. Singh, J. Feng, X. F. Shen, F. L. Cao, P. Oleynikov, H. Sun, O. Terasaki and S. N. Che, *Nat. Commun.*, 2014, **5**, 4262.
- 31 X. F. Shen, W. T. Mao, Y. H. Ma, D. D. Xu, P. Wu, O. Terasaki, L. Han and S. N. Che, *Angew. Chem.*, 2018, **130**, 732.
- 32 B. Li, Z. J. Hu, B. Kong, J. X. Wang, W. Li, Z. K. Sun, X. F. Qian, Y. S. Yang, W. Shen, H. L. Xu and D. Y. Zhao, *Chem. Sci.*, 2014, **5**, 1565.
- 33 A. J. J. Koekkoek, V. Degirmenci and E. J. M. Hensen, *J. Mater. Chem.*, 2011, **21**, 9279.
- 34 Y. H. Cheneviere, F. Chieux, V. Caps and A. Tuel, *J. Catal.*, 2010, **269**, 161.
- 35 Y. P. Guo, H. J. Wang, Y. J. Guo, L. H. Guo, L. F. Chu and C. X. Guo, *Chem. Eng. J.*, 2011, **166**, 391.
- 36 H. X. Tao, J. W. Ren, X. H. Liu, Y. Q. Wang and G. Z. Lu, *J. Solid State Chem.*, 2013, **200**, 179.
- 37 H. B. Zhu, E. A. Hamad, Y. Chen, Y. Saih, W. B. Liu, A. K. Samal and J. M. Basset, *Langmuir*, 2016, **32**, 2085.
- 38 B. L. Peng, H. B. Zou, L. P. He, P. M. Wang, Z. Q. Shi, L. K. Zhu, R. W. Wang and Z. T. Zhang, *CrystEngComm*, 2017, **19**, 7088.
- 39 M. R. Li, I. N. Oduro, Y. P. Zhou, Y. Hang and Y. M. Fang, *Microporous Mesoporous Mater.*, 2016, **221**, 108.
- 40 H. C. Xin, X. P. Li, L. Chen, Y. Huang, G. R. Zhu, X. B. Li and Energy Environ, *Focus.*, 2013, **2**, 18.
- 41 M. Milina, S. Mitchell, P. Crivelli, D. Cooke and J. Pérez-Ramírez, *Nat. Commun.*, 2014, **5**, 1.
- 42 N. B. Chu, J. H. Yang, C. Y. Li, J. Y. Cui, Q. Y. Zhao, X. Y. Yin, Y. M. Lu and J. Q. Wang, *Microporous Mesoporous Mater.*, 2009, **118**, 169.
- 43 Y.-S. Ooi, R. Zakaria, A. R. Mohamed and S. Bhatia, *Appl. Catal., A*, 2004, **274**, 15.
- 44 S. He, W. B. Zhang, D. G. Li, P. L. Li, Y. C. Zhu, M. M. Ao, J. Q. Li and Y. S. Cao, *J. Mater. Chem. B*, 2013, **1**, 1270.
- 45 Y. Xu, W. T. Chen, X. Y. Guo, Y. J. Tong, T. F. Fan, H. X. Gao and X. M. Wu, *RSC Adv.*, 2015, **5**, 52866.
- 46 B. Louis, F. Ocampo, H. S. Yun, J. P. Tessonnier and M. M. Pereira, *Chem. Eng. J.*, 2010, **161**, 397.
- 47 C. Wu, Y. Kong, F. Gao, Y. Wu, Y. N. Lu, J. Wang and L. Dong, *Microporous Mesoporous Mater.*, 2008, **113**, 163.
- 48 J. Wang, J. N. Park, X. Y. Wei and C. W. Lee, *Chem. Commun.*, 2003, 628.
- 49 M. N. Timofeeva, Z. Hasan, Y. A. Orlov, V. N. Panchenko, Y. A. Chesalov, I. E. Soshnikov and S. H. Jhung, *Appl. Catal., A*, 2011, **107**, 197.
- 50 Q. Wu, X. J. Hua, P. L. Yue, X. S. Zhao and G. Q. Lu, *Appl. Catal., B*, 2001, **32**, 151.